IL-6/STAT3 promotes regeneration of airway ciliated cells from basal stem cells

Tomomi Tadokoro[a], Yang Wang[b], Larry S. Barak[a], Yushi Bai[a], Scott H. Randell[b], and Brigid L. M. Hogan[a,1]

[a]Department of Cell Biology, Duke University Medical Center, Durham, NC 27710; and [b]Department of Cell Biology and Physiology, and Cystic Fibrosis/Pulmonary Research and Treatment Center, University of North Carolina at Chapel Hill, Chapel Hill, NC 27599

Edited by Kathryn V. Anderson, Sloan–Kettering Institute, New York, NY, and approved July 28, 2014 (received for review May 26, 2014)

The pseudostratified airway epithelium of the lung contains a balanced proportion of multiciliated and secretory luminal cells that are maintained and regenerated by a population of basal stem cells. However, little is known about how these processes are modulated in vivo, and about the potential role of cytokine signaling between stem and progenitor cells and their niche. Using a clonal 3D organoid assay, we found that IL-6 stimulated, and Stat3 inhibitors reduced, the generation of ciliated vs. secretory cells from basal cells. Gain-of-function and loss-of-function studies with cultured mouse and human basal cells suggest that IL-6/Stat3 signaling promotes ciliogenesis at multiple levels, including increases in multicilin gene and forkhead box protein J1 expression and inhibition of the Notch pathway. To test the role of IL-6 in vivo genetically, we followed the regeneration of mouse tracheal epithelium after ablation of luminal cells by inhaled SO_2. Stat3 is activated in basal cells and their daughters early in the repair process, correlating with an increase in *Il-6* expression in platelet-derived growth factor receptor alpha$^+$ mesenchymal cells in the stroma. Conditional deletion in basal cells of suppressor of cytokine signaling 3, encoding a negative regulator of the Stat3 pathway, results in an increase in multiciliated cells at the expense of secretory and basal cells. By contrast, *Il-6* null mice regenerate fewer ciliated cells and an increased number of secretory cells after injury. The results support a model in which IL-6, produced in the reparative niche, functions to enhance the differentiation of basal cells, and thereby acts as a "friend" to promote airway repair rather than a "foe."

epithelial repair | mucociliary epithelium | cell fate

The conducting airways of the human lung are lined by a pseudostratified epithelium composed of ciliated and secretory cells and basal stem cells. A similar epithelial architecture with basal cells is present in the mouse, although it is limited to the trachea and the largest bronchi. The integrity of this lining is vital for the process of mucociliary clearance by which multiciliated cells move mucus and trapped pathogens and particles out of the lung. Cellular turnover is low in the normal lung, but if luminal cells are destroyed by exposure to toxic compounds or pathogenic agents, the epithelium is rapidly restored from the basal cell population. An example of this injury/repair process is seen in the mouse trachea following exposure to inhaled SO_2. The surviving p63$^+$, Keratin-5 (K5)$^+$ basal cells quickly spread over the denuded basal lamina and proliferate and regenerate ciliated and secretory cells (1–4). Understanding the mechanisms driving this repair, including the role of factors produced by and acting in the local stem cell niche, may inform strategies to promote recovery after acute respiratory infections or damage by environmental agents. This knowledge may also inform strategies to treat conditions in which the turnover and composition of the airway epithelium are abnormal, for example, in goblet cell hyperplasia in asthma and chronic obstructive pulmonary disease (COPD) (5, 6).

Previous studies have identified transcription factors and signaling pathways that regulate the lineage choice of epithelial progenitors that have the potential to differentiate into either secretory or ciliated cells. One key regulator is the Notch signaling pathway. In the adult trachea, sustained Notch activation inhibits ciliogenesis and promotes the differentiation of basal cells into secretory cells (3). Notch signaling also inhibits ciliogenesis in the developing mouse lung, in human airway epithelium, and in the epidermis of *Xenopus* embryos (7–11). Other pathways acting downstream of Notch regulate the differentiation of progenitors into mature multiciliated cells. A critical transcriptional coregulator in this process is multicilin (Mcin or Mcidas), which coordinately controls centriole biogenesis and the assembly of cilia, as well as key transcription factors, such as Myb and forkhead box protein J1 (Foxj1) (12–14). Recent studies have also implicated microRNAs (miRNAs) of the miR-34/449 family in promoting ciliogenesis by suppressing multiple genes, such as *Notch1*, delta-like 1 (*Dll1*), and *Ccp110*, the latter of which is a centriolar protein that inhibits cilia assembly (10, 15, 16).

To identify additional factors regulating mucociliary differentiation, we developed a screen based on a 3D tracheosphere organoid system in which individual basal cells give rise to spheres containing ciliated and secretory luminal cells (4). Our findings revealed IL-6 and the downstream STAT3 pathway as positive regulators of multiciliogenesis. IL-6 functions by binding to IL-6 receptor subunit alpha (IL-6RA) and the coreceptor gp130, leading to the activation of JAK and the tyrosine phosphorylation of STAT3, which undergoes dimerization and nuclear translocation. One known direct target of phosphorylated STAT3 is suppressor of cytokine signals 3 (SOCS3), a negative feedback regulator that inhibits activation of the JAK/STAT3 pathway (17). Loss-of-function studies in the mouse have shown that STAT3 signaling is not essential for lung development. However, it is required for repair of the bronchiolar and alveolar regions after damage (18, 19), and transgenic overexpression of IL-6 in Club (previously, Clara) secretory cells results in bronchiolar

Significance

The airways of the lungs are lined by ciliated and secretory epithelial cells important for mucociliary clearance. When these cells are damaged or lost, they are replaced by the differentiation of basal stem cells. Little is known about how this repair is orchestrated by signaling pathways in the epithelium and underlying stroma. We present evidence using cultured airway cells and genetic manipulation of a mouse model of airway repair that the cytokine IL-6 promotes the differentiation of ciliated vs. secretory cells. This process involves direct Stat3 regulation of genes controlling both cell fate (Notch1) and the differentiation of multiciliated cells (Multicilin and forkhead box protein J1). Moreover, the major producer of IL-6 appears to be mesenchymal cells in the stroma rather than immune cells.

Author contributions: T.T., S.H.R., and B.L.M.H. designed research; T.T. and Y.W. performed research; L.S.B. and Y.B. contributed new reagents/analytic tools; T.T., Y.W., S.H.R., and B.L.M.H. analyzed data; and T.T. and B.L.H. wrote the paper.

The authors declare no conflict of interest.

This article is a PNAS Direct Submission.

Freely available online through the PNAS open access option.

[1]To whom correspondence should be addressed. Email: brigid.hogan@dm.duke.edu.

This article contains supporting information online at www.pnas.org/lookup/suppl/doi:10.1073/pnas.1409781111/-/DCSupplemental.

and alveolar abnormalities (20). However, none of these studies have addressed the role of IL-6/STAT3 signaling in the regions of the mouse lung that, like the intralobar airways of the human lung, are maintained by basal stem cells (21). Understanding the role of IL-6/STAT3 signaling in basal stem cells is important because IL-6 is up-regulated in asthma and COPD in humans and also in response to infections and damage by toxic agents (22), but the direct effect of the cytokine on airway repair has not been specifically tested. To address this question we used both gain-of-function and loss-of-function studies to explore the role of the IL-6/STAT3 pathway on human and mouse airway basal cells. Our results indicate that STAT3, activated by IL-6 produced by mesenchymal stromal cells after injury, promotes regeneration and multiciliogenesis through inhibition of the Notch pathway and direct regulation of genes, such as *Mcidas* and *Foxj1*. These data suggest that under some conditions, IL-6 produced locally in response to tissue damage plays a positive role in promoting airway repair from progenitor cells.

Results

Differentiation of Mouse Basal Progenitors into Ciliated Cells Is Stimulated by IL-6 and Inhibited by STAT3 Inhibitors. To screen rapidly for compounds regulating basal cell self-renewal and differentiation, we used a clonal tracheosphere culture assay (4) (Fig. 1*A*). To identify factors regulating ciliogenesis, we started with $p63^+$, $K5^+$, and NGF receptor ($NGFR^+$) basal cells from transgenic mice in which the promoter of *Foxj1*, a gene essential for the differentiation of multiciliated cells (23–25), drives the expression of EGFP (26). Cells were cultured in three dimensions using Matrigel (BD Biosciences) in the absence of stromal

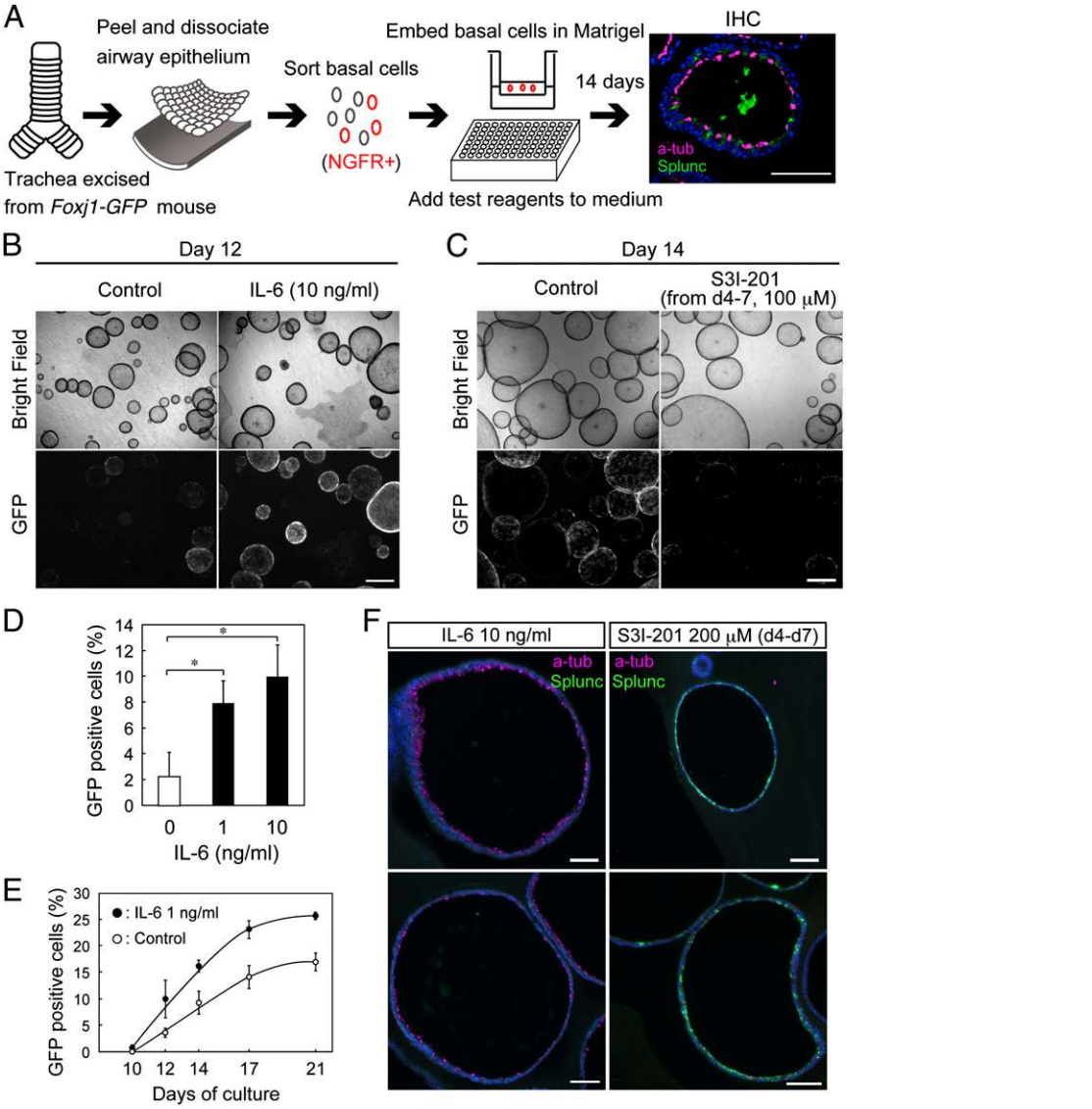

Fig. 1. IL-6 enhances *Foxj1-GFP* expression in the mouse tracheosphere culture assay. (*A*) Schematic of the assay. $NGFR^+$ basal cells from *Foxj1-GFP* tracheas were cultured in 50% Matrigel in 96-well inserts. (*Right*) Section of a typical sphere with acetylated tubulin$^+$ (a-tub) ciliated (magenta) and $Splunc^+$ secretory cells (green). IHC, immunohistochemistry. The effect of IL-6 (*B*) and STAT3 inhibitor (*C*) on *Foxj1*-GFP expression is shown. Differential interference contrast images (*Upper*) and fluorescent images (*Lower*) of the same spheres are shown. (*D*) Quantification by FACS at day 11 of the percentage of GFP^+ cells in dissociated spheres treated with IL-6 (0, 1, and 10 ng/mL). (*E*) Quantification at different times of GFP^+ cells in spheres cultured with or without IL-6 (1 ng/mL). (*F*) Representative sections of spheres at day 14 treated with IL-6 (*Left*, 10 ng/mL) or S3I-201 (*Right*, 200 μM, days 4–7). Both sections were stained with antibodies to a-tub$^+$ (magenta) and $Splunc^+$ (green). *$P < 0.02$ against control ($n = 3$). Error bars indicate SD ($n = 3$). (Scale bars: *A–C*, 500 μm; *F*, 100 μm.) (Also see Fig. S1.)

cells. Single factors were added at an initial concentration of 5 μM, and medium was changed every other day. At different times, up to 14 d, spheres were screened by fluorescence microscopy; the proportion of GFP$^+$ ciliated cells was then quantified by fluorescence-activated cell sorting (FACS) after dissociating spheres into single cells. Spheres were also fixed, sectioned, and stained with antibodies to acetylated tubulin (a marker for multiciliated cells) and Short palate, lung, and nasal epithelial clone (Splunc, a marker of secretory cells). We found that IL-6 enhances the proportion of *Foxj1-GFP*$^+$ cells in a dose-dependent manner while inhibiting the differentiation of Splunc$^+$ cells (Fig. 1 *B* and *D–F*). At low concentrations, IL-6 has no effect on colony-forming efficiency (CFE). At high concentrations, IL-6 inhibits CFE but still promotes ciliogenesis (Fig. 1*D* and Fig. S1*B*).

In contrast to the effect of IL-6, pyrimethamine [a compound that is reported to be a STAT3 inhibitor (27) and is present in the Johns Hopkins Clinical Compound Library (version 1.0)] had an inhibitory effect on the differentiation of *Foxj1-GFP*$^+$ cells (Fig. S1*A*). Inhibition of ciliogenesis, but not Splunc expression, was also seen with the STAT3 inhibitor, S3I-201 (Fig. 1 *C* and *F*). Because these inhibitors suppressed CFE when added from the beginning of the culture, spheres were treated with inhibitors only from days 4–7 (Fig. 1 *C* and *F*). Taken together, these results suggest that the IL-6/STAT3 pathway regulates the differentiation of basal progenitors into multiciliated cells vs. secretory cells.

Effect of IL-6 and Activated STAT3 on the Differentiation of Human Basal Cells in Air–Liquid Interface Culture. To determine whether the effect of IL-6 is conserved between mice and humans, we used primary human bronchial epithelial (HBE) cells cultured at the air–liquid interface (ALI) in the absence of stromal cells. Under these conditions, p63$^+$ basal cells self-renew and differentiate into ciliated and secretory cells (28) (Fig. 2*A*). As described previously, the kinetics and absolute levels of differentiation achieved over the 21-d culture period vary between individual donors. Under the condition used in this study, ALI cultures at day 21 contain 6.0 ± 1.8% ciliated cells (n = 9 individual donors). However, IL-6 reproducibly gave a dose-dependent increase in the proportion of multiciliated cells to 19.4 ± 4.3% (n = 9) (Fig. 2 *B* and *C* and Fig. S2*A*). By contrast, there was a significant decrease in the proportion of cells staining for secretoglobin 3A1 (SCGB3A1), a product of secretory cells (Fig. 2 *B* and *C*). These results were also confirmed by quantitative PCR (qPCR) for *FOXJ1*, *SNTN* (encoding a structural protein in cilia), and *SCGB3A1* (Fig. S2*C*). There was also a significant decline in the proportion of basal cells (Fig. S2 *D* and *E*). No difference was seen in cell proliferation at this or an earlier time (3, 7, or 14 d) (Fig. S2*B*).

STAT3 Regulates Ciliogenesis Through Its Phosphorylation. To determine whether the effect of IL-6 is mediated by the JAK/STAT3 pathway, we carried out gain-of-function and loss-of-function studies by infecting mouse ALI cultures with lentivirus expressing constitutively active *Stat3* (ca*Stat3*)-P2A-*RFP*, dominant-negative *Stat3* (dn*Stat3*)-P2A-*RFP*, or control virus (RFP only). caSTAT3 mimics the protein dimer that normally forms following phosphorylation of tyrosine 705, whereas dnSTAT3 has a mutation at tyrosine 705 that prevents phosphorylation and inhibits dimer formation (29). Mouse tracheal epithelial cells from *Foxj1-GFP* mice were seeded on an insert and infected with lentivirus at day 3. After transfer to ALI culture at day 4, the cells start to differentiate into ciliated and secretory cells (30) (Fig. 3*A*). At day 12, 82.3 ± 6.4% of cells infected with ca*Stat3*-P2A-*RFP* virus (marked by RFP) express *Foxj1-GFP* compared with only 18.8 ± 2.1% of the cells infected with control virus. For cells infected with dn*Stat3*-P2A-*RFP*, the corresponding value was 2.4 ± 2.1% (Fig. 3 *B* and *C*). These results indicate that activation of STAT3 through tyrosine phosphorylation in basal cells and/or their descendants positively regulates the expression of *Foxj1* and ciliogenesis.

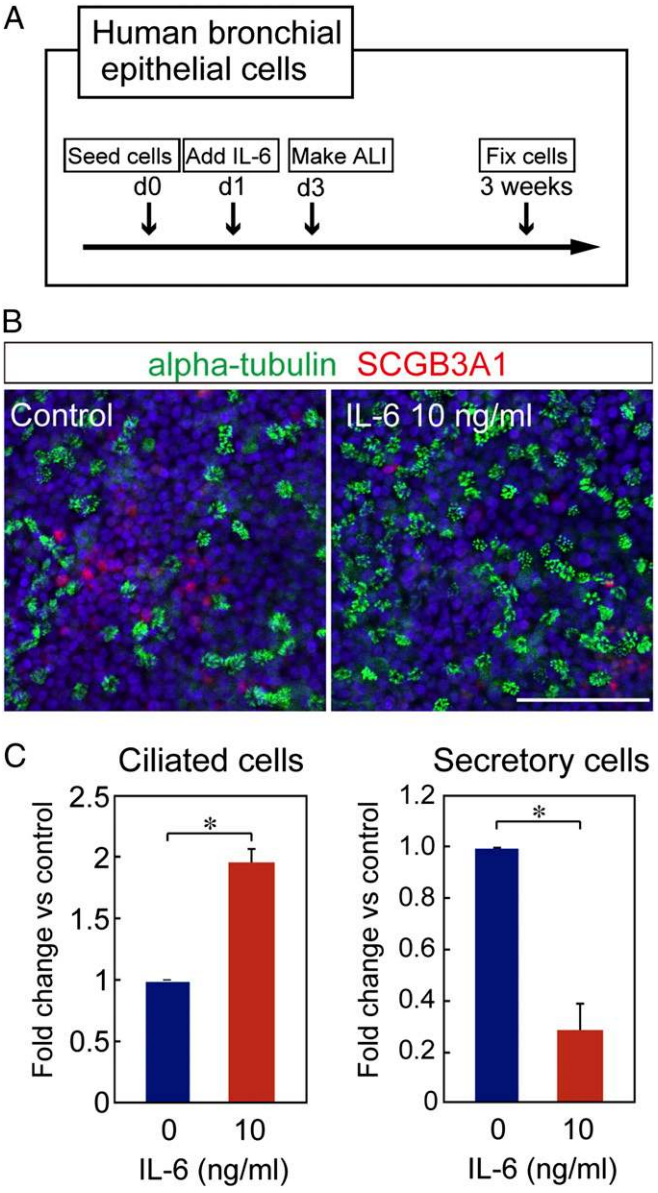

Fig. 2. Effect of IL-6 on regeneration of human epithelium in ALI culture. (*A*) Schematic of ALI culture of primary HBE cells. (*B*) Whole-mount staining of day 21 cultures for ciliated (α-tubulin, green) and secretory (SCGB3A1, red) cells. Nuclei are blue (DAPI). (Scale bar: 100 μm.) (*C*) Quantification of whole-mount staining, shown as a fold change over untreated culture. The α-tubulin$^+$ or SCGB3A1$^+$ cells were counted in four randomly chosen areas (0.18 mm^2) per filter. Values are mean ± SD for cultures from three different donors. *$P < 0.001$ against control (n = 3). Error bars indicate SD (n = 3). (Also see Fig. S2.)

STAT3 Promotes Ciliogenesis Through Inhibition of Notch Signaling and Activation of Ciliogenesis-Related Genes. To clarify the mechanism by which STAT3 promotes ciliogenesis, we used qPCR to examine gene expression changes in mouse ALI cultures after IL-6 treatment. Cells were treated with IL-6 (10 ng/mL) on day 7 of culture and harvested 6, 12, and 24 h after treatment (Fig. 4*A*). Gene expression levels were normalized to *Gapdh*, and *Socs3* was used as a positive control (Fig. 4*B*). *Foxj1* and *Mcidas*, known regulators of ciliogenesis (12, 13), were both up-regulated in response to IL-6 (Fig. 4*B*). Among components of the Notch signaling pathway, which negatively regulates ciliogenesis (10, 11, 31), *Notch1* transcripts were down-regulated, whereas *Notch2*,

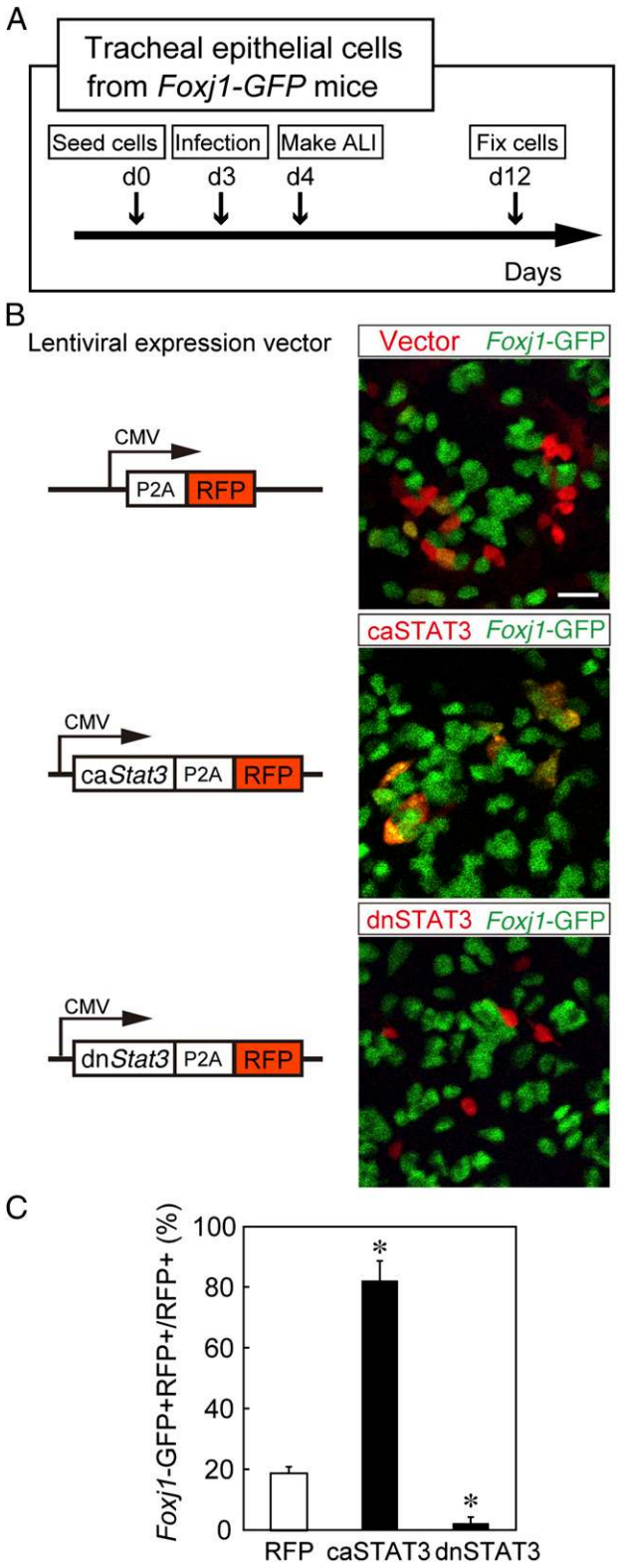

Fig. 3. STAT3 pathway regulates ciliogenesis in mouse epithelium in ALI culture. (*A*) Schematic of ALI culture of mouse tracheal epithelial cells. Subconfluent cultures are infected with lentivirus at day 3 when cells are undifferentiated. (*B*) Virus-infected cells are RFP$^+$ (red), and *Foxj1*-expressing cells are GFP$^+$ (green). The caSTAT3 promotes ciliogenesis (*Middle*), but the dnSTAT3 inhibits ciliogenesis (*Bottom*) compared with control (*Top*). (Scale bar: 20 μm.) (*C*) Quantification of results in *B*. *$P < 0.001$ against control ($n = 3$). Error bars indicate SD ($n = 3$).

Dll1, and *Jagged1* were not changed (Fig. 4*B*). By contrast, the transcription of *Cdc20b*, which encodes a ciliogenesis-related miRNA, miR-449a/b, was up-regulated in both mouse cells (Fig. 4*B*) and HBE cells in ALI (Fig. S2*F*). Taken together, these results suggest that IL-6 promotes the differentiation of basal cells into multiciliated cells by down-regulating the Notch signaling pathway and up-regulating ciliogenesis genes.

Previous studies showed that the cytokine IL-13, which reduces ciliogenesis and promotes secretory cell differentiation in airway epithelium (32), inhibits *Foxj1* transcription directly through STAT6 binding to a target site in the *Foxj1* promoter (33). *Mcidas* and *Notch1* also have putative STAT3 binding sites in their promoter regions. We therefore used a ChIP assay with antibody to phospho-STAT3 (p-STAT3) to ask whether activated STAT3 directly regulates *Notch1*, *Mcidas*, and *Foxj1* (Fig. 4*C*). IL-6 was added to cells in ALI culture at day 7, and samples were harvested for ChIP analysis 4 h later. The result showed that p-STAT3 binding to promoter regions of *Foxj1*, *Mcidas*, *Notch1*, and *Socs3* (the positive control) was increased after IL-6 stimulation (Fig. 4*C*). This suggests that IL-6/STAT3 modulates ciliogenesis through direct regulation of *Notch1*, *Mcidas*, and *Foxj1*.

Expression of IL-6 and Activated STAT3 During Airway Repair. We next asked whether the activity of the IL-6/STAT3 pathway changes in vivo during the repair of adult tracheal epithelium after SO_2 injury. In this model (Fig. 5*A*), luminal cells die and surviving K5$^+$ p63$^+$ basal cells spread to cover the denuded basal lamina and proliferate to give rise to a population of undifferentiated luminal cells that are K8$^+$, K5$^-$, p63$^-$, FOXJ1$^-$, and SCGB1A1$^-$ (termed "undifferentiated progenitors" here) (3). FOXJ1$^+$ cells and cells expressing the secretory marker SCGB3A2 can be detected from 3 d postinjury (dpi) (Fig. 5*C*), and SCGB1A1$^+$ secretory cells and multiciliated cells are observed from 5 dpi, with repair complete in 2 wk. Using immunohistochemistry, we observed p-STAT3 in basal cells (p63$^+$) and undifferentiated progenitors at 24 and 48 h postinjury (hpi) (Fig. 5*B*). At these two times, p-STAT3$^+$ cells made up 68.4% and 56.4% of the total, respectively. Although the overall proportion of positive cells subsequently declined, at 3 dpi, 51.5% of the FOXJ1$^+$ cells are p-STAT3$^+$.

Several cytokines can activate JAK/STAT3 signaling downstream of gp130, including IL-6, IL-11, IL-10, leukemia inhibitory factor (LIF), oncostatin-M (OSM), and ciliary neurotrophic factor (CNTF) (34). We therefore examined levels of transcripts for these cytokines in the trachea at different times after SO_2 injury. *Il-6* transcripts showed a transient 150-fold increase at 24 hpi compared with steady state (Fig. 6*A*), and in situ hybridization revealed these transcripts in the stroma beneath the epithelium, particularly in the intercartilage regions (Fig. 6*B*). By contrast, there was only a slight transient increase in *Il-11* and *Osm* at 24 hpi (fourfold and threefold, respectively) and no changes in the levels of *Cntf*, *Lif*, and *Il-10* (Fig. 6*A*). In other tissues, epithelial repair is frequently associated with the transient influx of immune cells (35), and we confirmed the influx for the SO_2 injury model, with significant changes in the proportion of monocytes and neutrophils at 24 hpi and macrophages and neutrophils at 48 hpi (Fig. S3 *A* and *B*). The mesenchyme also contains numerous resident stromal cells that express platelet-derived growth factor receptor alpha (PDGFRα), as shown by the expression of histone H2B/GFP from a knock-in reporter allele (36) (Fig. 6*D*). When the levels of *Il-6* transcript were measured by qPCR in different cell populations isolated by FACS, the highest relative expression was seen in the *Pdgfrα*-GFP$^+$ stromal cells compared with different immune cells (Fig. 6*C*). Localization of *Il-6* transcripts in these cells was confirmed by in situ hybridization of tracheal sections (Fig. 6*E*). These results suggest that the stromal cells are a major source of IL-6 during repair.

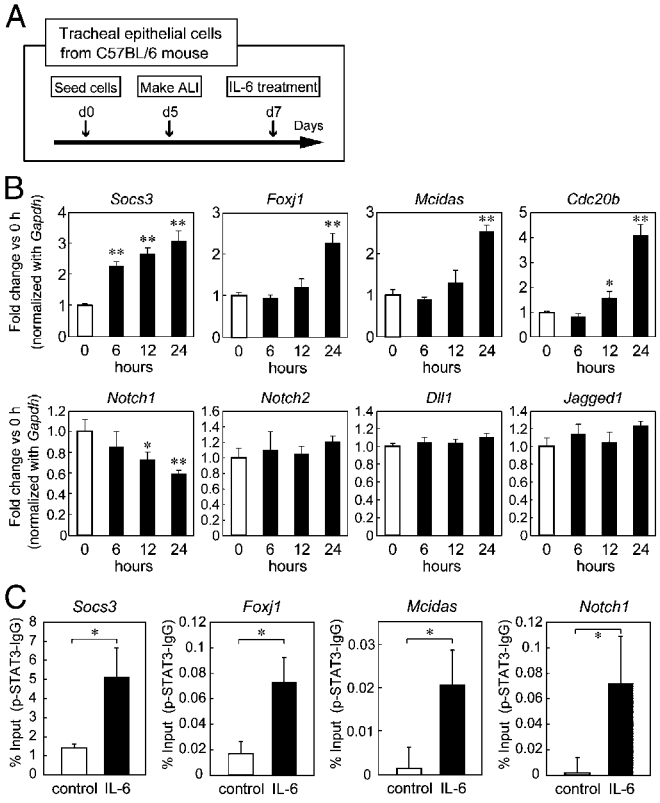

Fig. 4. IL-6 enhances expression of cilia-related genes and inhibits Notch1 expression in mouse ALI culture. (*A*) Schematic of ALI culture of mouse tracheal epithelial cells. At day 7, IL-6 (10 ng/mL) was added to culture medium in the lower chamber. Cells were harvested after 6, 12, and 24 h, and total RNA was extracted. (*B*) Quantitative RT-PCR shows that IL-6 treatment promotes the expression of the known target gene *Socs3* and ciliogenesis-related genes, such as Multicilin (*Mcidas*) and *Foxj1*. IL-6 treatment also inhibits *Notch1* and promotes expression of *Cdc20b*, the host gene for miR-449a/b. No significant changes were observed in the expression of *Notch2*, *Dll1*, or *Jagged1*. (*C*) ChIP assay shows that p-STAT3 binding to promoter regions of *Socs3, Foxj1*, *Mcidas*, and *Notch1* is increased after IL-6 stimulation. $*P < 0.05$ against control; $**P < 0.001$ against control ($n = 3$). Error bars indicate SD ($n = 3$).

IL-6 and STAT3 Regulate Differentiation of Basal Cells During Repair in Vivo. To examine the in vivo role of the IL-6/STAT3 signaling pathway further, we carried out genetic gain-of-function and loss-of-function experiments in the mouse. For gain-of-function experiments, we made use of a K5-CreER (*K5-CreER^{T2}*) knock-in allele that drives recombination specifically in basal cells. We also exploited the fact that SOCS3 is a feedback inhibitor specifically of the JAK/STAT3 pathway (Introduction). Administration of tamoxifen (Tmx) to *K5-CreER^{T2}; Socs3$^{flox/flox}$; Rosa-YFP* mice both deleted *Socs3* in basal cells and activated YFP expression as a lineage trace (Fig. 7*A*). *K5-CreER^{T2}; Rosa-YFP* mice were used as controls. After three doses of Tmx, mice were treated with SO_2 for 4 h (Fig. 7*A*). In the *Socs3* conditional KO mice, sustained activation of STAT3 was observed at 6 dpi; however, in control mice, pSTAT3 was no longer seen at this time (Fig. S4*A*). Tracheas were harvested at 6 dpi, and longitudinal sections were stained with GFP antibody and cell-specific markers to define cell types. Even though the overall level of recombination is quite low with our *K5-CreER^{T2}* allele (about 25%), gain-of-function experiments result in a 33% increase in the proportion of ciliated cells, from 21.4 ± 2.4% in controls to 30.8 ± 0.7% in conditional mutants (Fig. 7 *B* and *C*) ($n = 3$; $P < 0.01$). At the same time, there was a decrease in the proportion of basal cells, from 47.6 ± 3.5% to 37.9 ± 3.0%, and in SCGB1A1 secretory cells, from 26.6 ± 2.5% to 18.4 ± 2.4% ($n = 3$) (Fig. 7*C*). Similar results were observed when SCGB3A2 was used to score secretory cells (11.9 ± 0.8% in Stat3 gain-of-function mice compared with 21.7 ± 1.6% in controls, $n = 3$) (Fig. 7*C*).

For loss-of-function genetic experiments, we compared the response to SO_2 injury in WT vs. *Il-6* null mutant (KO) mice. At 4 dpi, the percentage of FOXJ1$^+$ cells in the tracheal epithelium of *Il-6* KO mice was reduced by 35%, from 26.8 ± 3.9% in WT mice to 17.3 ± 2.4% in mutants ($n = 3$, $P = 0.02$). On the other hand, the percentage of SCGB3A2$^+$ cells was increased by 44%, from 14.3 ± 2.4% in WT mice to 20.6 ± 1.6% in mutants ($n = 3$, $P = 0.02$) (Fig. 7 *D–F*). These results were also confirmed by qPCR for both genes (Fig. S4*B*). These results are consistent with a model in which JAK/STAT3 signaling downstream of IL-6 regulates the differentiation of multipotent basal cells toward ciliated cells during repair in vivo.

Discussion

An important goal in regenerative biology is to define the mechanisms by which cytokines, growth factors, and other effector molecules produced locally in damaged tissues influence the self-renewal and differentiation of resident stem and pro-

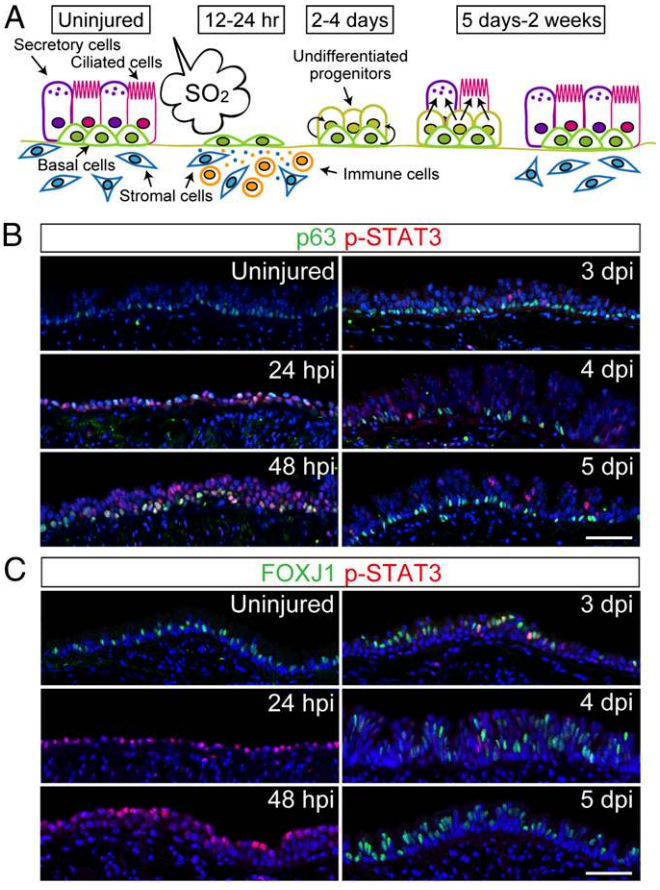

Fig. 5. IL-6/STAT3 signaling is activated in tracheal epithelium during repair. (*A*) Schematic of the SO_2 injury model. After exposure to SO_2, luminal cells die. Basal cells spread, proliferate, and generate early progenitors. These progenitors differentiate into ciliated and secretory cells, and repair is complete in 2 wk. (*B*) Longitudinal midline sections stained with antibodies to p-STAT3 (red) and p63 (green), a marker for basal cells. (*C*) Expression of p-STAT3 (red) and FOXJ1 (green) during epithelial repair. Note the coexpression of p-STAT3 and FOXJ1 at 3 dpi. (Scale bars: *B* and *C*, 50 μm.) (Also see Fig. S3.)

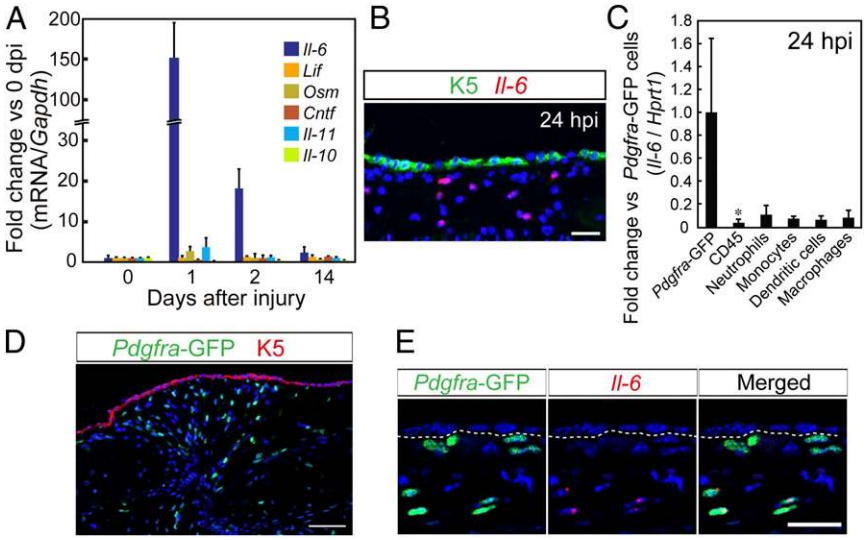

Fig. 6. IL-6 is up-regulated in PDGFRα$^+$ stromal cells after SO_2 injury. (*A*) RNAs were extracted from whole trachea at 0, 1, 2, and 14 d after injury and subjected to quantitative RT-PCR analysis. The mRNA expression level of cytokines was normalized to *Gapdh*. (*B*) In situ hybridization combined with immunohistochemistry shows that *Il-6* mRNA (red) is expressed in cells in the stroma beneath basal cells (K5$^+$, green) after SO_2 injury. (*C*) Quantitative PCR analysis of *Il-6* expression in sorted stromal cells [*Pdgfrα* (*Pdgfra*)-GFP$^+$] and immune cell subpopulations from the trachea at 24 hpi. (*D*) Immunohistochemistry of a trachea section at 24 hpi shows *Pdgfra*-GFP$^+$ cells (GFP$^+$, green) in the stroma beneath the epithelium with basal cells (K5$^+$, red). (*E*) In situ hybridization and immunohistochemistry show that *Pdgfra*-GFP$^+$ cells (GFP$^+$, green) express *Il-6* mRNA (red) at 24 hpi. (Scale bars: *B* and *E*, 20 μm; *D*, 50 μm.) *$P < 0.05$ against control ($n = 3$). Error bars indicate SD ($n = 3$).

genitor cells. Because multiple factors are usually produced in response to injury by resident epithelial and stromal cells, as well as by immune cells summoned to the site of action, it is important to parse out the likely contribution of each and to determine whether each is acting as "friend" or "foe" in the repair process. Here, we provide multiple lines of evidence that the IL-6/IL-6RA/JAK/STAT3 signaling pathway, a pathway that has been shown to exert either proinflammatory or anti-inflammatory effects in other systems depending on the in vivo context (37, 38), can play a positive role in the regeneration of the mucociliary airway epithelium from basal stem cells and promote the differentiation of ciliated vs. secretory cells.

The function we have uncovered here in the mouse tracheal epithelium and primary HBE cells can be compared with the role of the *Drosophila* IL-6 homolog, Unpaired (Upd1, Upd2, and Upd3) and its receptor, Domed, in regulating the behavior of adult midgut intestinal stem cells (ISCs). Upd ligands can be produced by either visceral muscle cells in steady state or luminal cells following bacterial infection or tissue damage. In both cases JAK-STAT signaling is activated in ISCs and enteroblasts to enhance, through the Notch pathway, their differentiation into enterocytes (39–41). Fig. 8 summarizes our current model for how IL-6/STAT3 regulates ciliogenesis in the mouse trachea following damage and loss of luminal cells in response to SO_2. In this model, the stromal cell population secretes IL-6, and multiple cell types, including p63$^+$ basal cells, undifferentiated progenitors, and FOXJ1$^+$ precursors of ciliated cells, respond, as judged by their expression of nuclear p-STAT3, at different times during the repair process (Fig. 5 *B* and *C*). Our studies suggest that Stat3 signaling functions at two levels: (*i*) in basal cells and early progenitors to inhibit secretory and promote ciliated fate by directly inhibiting Notch 1 gene expression and (*ii*) in ciliated progenitors to promote differentiation and cilia biogenesis through up-regulating *Mcidas, Foxj1*, and *Cdc-20b/miR-449*. Further studies will be needed to define the complete spectrum of direct transcriptional targets in basal cells and undifferentiated progenitors that promote ciliogenesis (42). Finally, it is likely that factors other than IL-6 promote ciliogenesis in vivo, an assumption based on the fact that the level of Foxj1$^+$ cells was only reduced by about 35% during repair in *Il-6* null mice. These other factors may be members of the IL-6 family of cytokines, albeit produced at lower levels in the model system used here, or they could be other regulators that are yet to be identified.

In this paper, we have focused on the role of IL-6/STAT3 signaling in the regeneration of the mucociliary epithelium from basal progenitors. The response to IL-6, namely, an enrichment of ciliated cells in the epithelium, makes biological sense because it likely enhances the clearance of noxious material from the airways. The increased expression of IL-6 observed in patients suffering from chronic respiratory disorders, such as asthma, COPD, and emphysema (22), may thus reflect attempts by the tissue to restore a functional epithelium from basal progenitors in the face of repeated shedding or loss of luminal cells (43). Such a potentially positive, rather than negative, role of IL-6 in homeostasis and repair should be born in mind when proposing therapeutic drug strategies to block IL-6 signaling in patients with asthma who carry variant alleles of *IL-6R* (44, 45). Finally, our results suggest that IL-6 may help to promote the differentiation of functional mucociliary epithelium from pluripotent stem cells for drug screening or for bioengineering replacement parts. In other endodermal tissues, the final maturation of specialized cell types has proved to be a roadblock to clinical translation.

Materials and Methods

Animals. *Socs3*^{flox} mice (46) were provided by Douglas Hilton, The Walter and Eliza Hall Institute of Medical Research, Parkville, Australia. *Socs3*^{flox} (46), *K5-CreER*^{T2} (47), *Rosa-YFP* (48), *Foxj1-GFP* (26), and *Pdgfrα-H2B:GFP* mice (36) were maintained on a C57BL/6 background. B6.129S2–*Il-6*^{tm1Kopf}/J null mutant mice were maintained as homozygotes. Male mice 8–12 wk old were given three doses of Tmx (0.1 mg/g of body weight) through oral gavage every other day. One week after the final dose, mice were exposed to 500 ppm of SO_2 in air for 4 h. All experiments were approved by the Duke Institutional Animal Care and Use Committee.

Tracheosphere Culture. NGFR$^+$ basal cells (4) from *Foxj1-GFP* mice were suspended in mouse tracheal epithelial cells (MTEC)/plus medium (30), mixed at a 3:7 ratio with growth factor-reduced Matrigel (BD Biosciences), and seeded

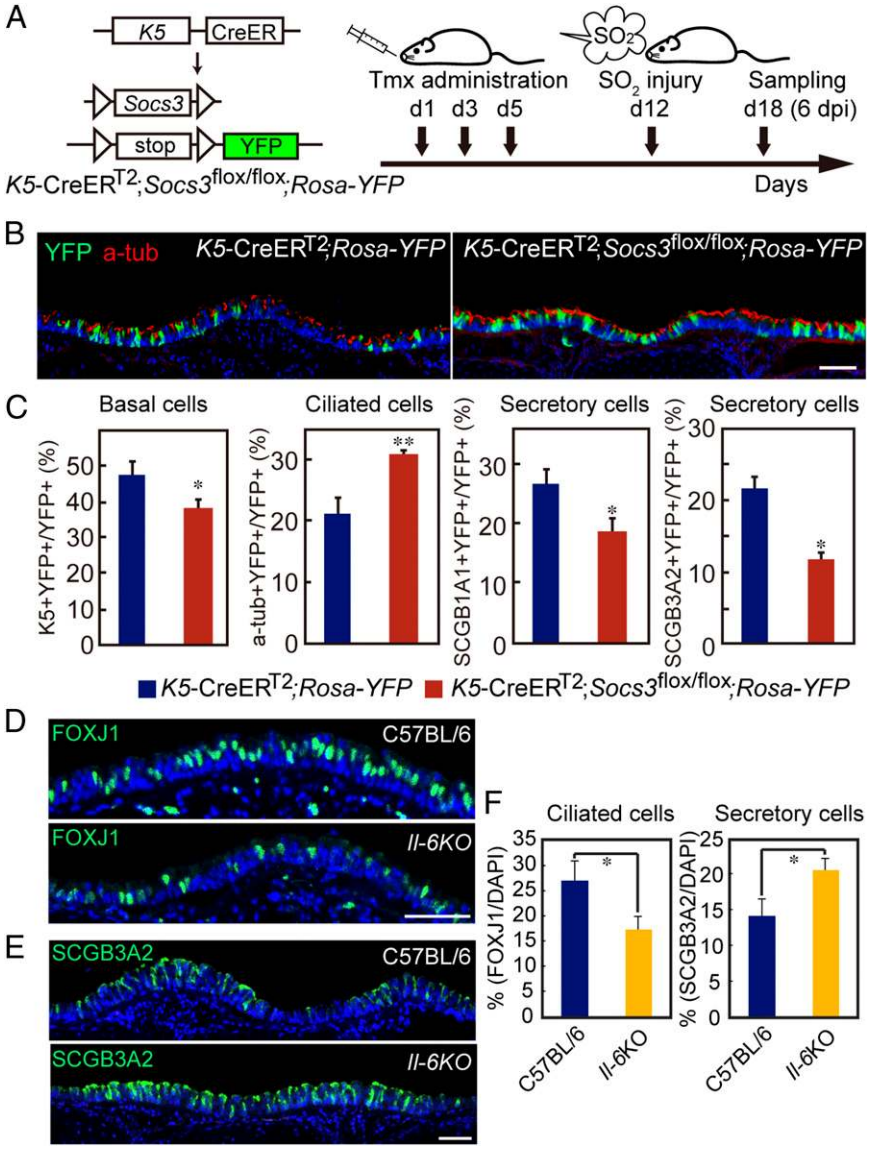

Fig. 7. Effect of IL-6/STAT3 on tracheal epithelial repair in vivo. (*A*) Schematic of gain-of-function (*K5-CreER^{T2}; Socs3$^{flox/flox}$; Rosa-YFP*) model. Floxed alleles are deleted, and the YFP reporter is activated in basal cells with three doses of Tmx. One week later, mice are exposed to SO_2 and tracheas are harvested at 6 dpi. (*B*) Representative midline sections of tracheas (ventral) stained with YFP (lineage label, green) and a-tub (ciliated cells, red) in control (*K5-CreER^{T2}; Rosa-YFP*) and gain-of-function (*K5-CreER^{T2}; Socs3$^{flox/flox}$; Rosa-YFP*) mice. A similar analysis was carried out using antibodies to K5 for basal cells and SCGB1A1 and SCGB3A2 for secretory cells, respectively. (*C*) Percentage of total lineage-labeled cells (YFP$^+$) throughout the trachea that are ciliated, secretory, or basal cells. Blue and red bars show *K5-CreER^{T2}; Rosa-YFP* and *K5-CreER^{T2}; Socs3$^{flox/flox}$; Rosa-YFP*, respectively. (*D*) FOXJ1 staining (green) of airway epithelium at 4 dpi in WT and *Il-6* null mice. (*E*) SCGB3A2 staining (green) of airway epithelium at 4 dpi in WT and *Il-6* null mice. (*F*) In *Il-6* null mice, there is a reduction of ciliated cells (FOXJ1$^+$) and an increase of secretory cells (SCGB3A2$^+$) after SO_2 injury (4 dpi). *$P < 0.05$ against control; **$P < 0.001$ against control ($n = 3$). Error bars indicate SD ($n = 3$). (Scale bars: 50 μm.) (Also see Fig. S4.)

at 333 cells per well in 96-well, 1-μm pore inserts (Falcon) coated with 5 μL of 100% Matrigel. Medium in the lower well was changed every other day. MTEC/serum free (SF) (30) was used from day 7. Images were taken using an AxioVert 200 M microscope (Carl Zeiss). For quantifying GFP$^+$ cells, spheres were dissociated with dispase and 0.1% trypsin/EDTA, fixed with 2% (wt/vol) paraformaldehyde (PFA) in PBS, and then analyzed using a FACSCanto (BD Biosciences). For immunohistochemistry, spheres were fixed with 4% (wt/vol) PFA in PBS for 30 min and then embedded in 3% (wt/vol) agarose, followed by embedding in paraffin. For statistical analyses, three independent experiments were done in triplicate.

Human ALI Culture. Primary human tracheobronchial epithelial cells were obtained from excised subtransplant-quality lungs under a University of North Carolina Biomedical Institutional Review Board-approved protocol (03-1396) as previously described (28), and informed consent from patients was obtained. Passage 2 cells were seeded at 2.0×10^5 cells per insert on collagen IV-coated, 10-mm diameter Millicell CM 0.4-μm pore-sized inserts (Millipore) or in 6.5 mm of Transwell with 0.4-μm pore-sized inserts (Corning). IL-6 was added from day 1, and the medium was changed every 2–3 d. When cells reached confluence, the apical medium was removed with basolateral feeding only, and apical washing was performed with PBS once per week. Cells were harvested for RNA, and membranes were fixed for histological/immunocytochemical analysis at the times indicated. Cells were stained by antibody for α-tubulin or SCGB3A1 antibody with DAPI, and images were taken by confocal microscopy (49). For quantification, α-tubulin or SCGB3A1$^+$ cells were counted in four randomly chosen areas (425 μm × 425 μm, 0.18 mm^2 per area), except for the area within 1 mm from the edge of the well. Statistical analyses were done using results from three different donors.

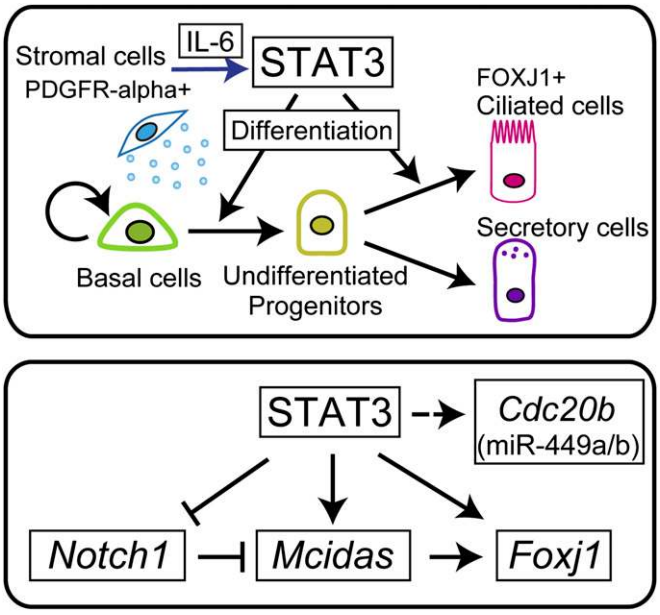

Fig. 8. Model for regulation of ciliogenesis in airway epithelium by STAT3. (*Upper*) After injury, STAT3 in both basal cells and progenitors is activated by IL-6 secreted from PDGFRα^+ stromal cells. Ciliogenesis is likely promoted both at the level of cell fate determination and at the level of differentiation/maturation of the progenitors of multiciliated cells. (*Lower*) Schematic model for how STAT3 may directly regulate ciliogenesis-related genes during repair of the tracheal epithelium.

Immunohistochemistry. Mouse tracheas were fixed with 4% (wt/vol) PFA in PBS at 4 °C for 4 h, washed with PBS, and processed for frozen or paraffin-embedded sectioning. Tracheas were sectioned longitudinally in the midline along the dorsal-ventral axis at 12 μm (frozen) or 7 μm (paraffin-embedded). Paraffin sections were deparaffinized, rehydrated, and steamed with sodium citrate (pH 6.0) at 121 °C for 10 min. After blocking with 10% (vol/vol) donkey serum, 3% (wt/vol) BSA, and 0.1% Triton X-100 in PBS, samples were incubated with primary antibodies in blocking buffer at 4 °C overnight. Primary antibodies used were as follows: rabbit K5 (1:1,000; Covance), mouse p63 (1:100, 4A4; Santa Cruz Biotechnology), rabbit p-STAT3 (Tyr705; 1:200, 9145; Cell Signaling Technology), mouse FOXJ1 (1:1,000; eBioscience), mouse a-tub (1:1,000, T7451; Sigma), rabbit Splunc (1:750, a gift from Colin Bingle, University of Sheffield, Sheffield, United Kingdom), rat α-tubulin (1:400; Millipore), mouse Muc5Ac (1:1,000; Thermo Fischer Scientific), goat SCGB1A1 (1:10,000, a gift from Barry Stripp, Cedars Sinai Medical Center, Los Angeles, CA), mouse SCGB3A1 (1:100; R&D Systems), rabbit SCGB3A2 (1:500, a gift from Shioko Kimura, National Cancer Institute, Bethesda, MD), and chicken GFP (1:500, GFP1020; Aveslab). Unless otherwise stated, Alexa Fluor-labeled secondary antibodies (Invitrogen) were used at a 1:500 dilution. Alexa488-labeled donkey anti-rat IgG (H+L, 1:500), Alexa488-labeled donkey anti-chicken IgY (1:500), and cyanine 3 (Cy3)-labeled donkey anti-mouse IgG (H+L, 1:500) were purchased from Jackson ImmunoResearch. After washing with PBS, nuclei were stained with DAPI and mounted in FluoSaver (Calbiochem). Confocal images were obtained using an LSM 710 inverted confocal microscope (Carl Zeiss). For quantification, images between cartilages 2 and 10 were tiled, and cells were counted on dorsal and ventral surfaces and averaged from three sections from three different tracheas.

Mouse ALI Culture and Virus Infection. The ca*Stat3* (A661C and N663C) and dn*Stat3* (Y705F) vectors were from Addgene (13373 and 8709) (50, 51). The lentiviral vector (Lenti-FCMV-P2A-*EGFP* W; a gift from Fan Wang, Duke University) was modified by replacing *GFP* with *RFP*. Genes were cloned into BamHI and NheI sites. Expression vector and packaging vectors (Δ8.9 and VSVg) were transfected into 293T cells using Lipofectamine 2000 (Invitrogen), and medium was collected twice every 24 h. Viruses were centrifuged at 65,000 × *g* ta 4 °C for 2.5 h and suspended in HBSS. Mouse tracheal epithelial cells were dissociated with 0.1% trypsin/EDTA and seeded on rat tail collagen I-coated, 24-well 0.4-μm inserts at 7.5×10^4 cells per insert. Medium was changed every other day. Lentivirus was added on top at day 3. When cells reached confluence, the overlying medium was removed and the medium in the well was changed to MTEC/SF (30). At day 12, cells were fixed, stained, and observed by confocal microscopy. For quantitative RT-PCR analysis, cells were stimulated with IL-6 (10 ng/mL) at day 7 and were harvested at the times indicated. Statistical analysis was done using results from three independent experiments.

Quantitative RT-PCR. Total RNA was extracted from cells or whole tracheas using an RNeasy kit (Qiagen). cDNA was synthesized using SuperScript III reverse transcriptase (Invitrogen), and quantitative RT-PCR was performed with iQ SYBR Green Supermix (Bio-Rad) using a StepOne Plus System (Applied Biosystems). Primer sequences are listed in Table S1. For miRNA, RNAs were extracted using the mirVana miRNA Isolation Kit (Life Technologies), and qRT-PCR was performed with a TaqMan MicroRNA Reverse Transcription Kit and TaqMan Universal PCR Master Mix (both from Invitrogen). Human miRNA-449a and the control *RPL21* were analyzed using a TaqMan MicroRNA Assay from Invitrogen (nos. 001030 and 001209, respectively). For quantitative RT-PCR from mouse ALI culture, statistical analysis was done using results from three independent experiments. For human ALI culture and mouse trachea experiments, statistical analyses were done using results from three different donors or three different mice.

ChIP Analysis. Mouse ALI cultures at day 7 were exposed to mouse IL-6 (20 ng/mL; R&D Systems) at 37 °C for 4 h. Approximately 4×10^6 cells were fixed at room temperature for 10 min and scraped off the inserts. The ChIP assay was performed using a SimpleChIp Enzymatic Chromatin IP Kit (Cell Signaling Technology) following the manufacturer's instructions. In brief, nuclei were digested by micrococcal nuclease, followed by sonication. Chromatin was precipitated with rabbit p-STAT3(Y705) antibody (9145; Cell Signaling Technology) or rabbit control IgG. Purified DNA samples were analyzed by qPCR and were normalized with input DNA. The primers used for STAT binding sites in the respective promoter regions were as follows: 5′-CACAGCCTTTCAGTGCAGAG-3′ and 5′-GTATTTACCCGGCCAGTACG-3′ for *Socs3*, 5′-GCTGGCTCTGCTTCCTAGAC-3′ and 5′-GTAGGGTAACCCAGCGTCTC-3′ for *Foxj1*, 5′-CTGGCTTCAGTACTCTGCTTCA-3′ and 5′-TGCCAAAGCTCTGCTCTGTA-3′ for *Mcidas*, and 5′-CTGTAACCCAAGCCCTGATTTCC-3′ and 5′-CACGGGATGGCTTCTCACTG-3′ for *Notch1*. Statistical analysis was done using results from three independent experiments.

In Situ Hybridization. Paraffin sections were deparaffinized and rehydrated, and then treated with Proteinase K (50 μg/mL; Invitrogen) for 10 min, followed by acetylation with triethanolamine for 10 min at room temperature. After prehybridization, digoxigenin (DIG)-labeled probes (500 ng/mL) were hybridized at 65 °C overnight. After washing once with 5× SSC and four times with 0.2× SSC at 65 °C, slides were blocked with 10% (vol/vol) heat-inactivated sheep serum in Tris-buffered saline for 1 h and incubated with alkali phosphatase-conjugated sheep anti-DIG antibody (1:1,000; Roche Applied Science) in 1% heat-inactivated sheep serum/PBS at 4 °C for overnight. To detect K5 or GFP, slides were incubated with anti-K5 antibody or anti-GFP antibody, followed by secondary antibody with DAPI for counterstaining (*Materials and Methods*, *Immunohistochemistry*). Slides were incubated with FastRed (Roche Applied Science) for 2–3 h to develop color.

Flow Cytometric Analysis and Cell Sorting. For analysis of immune cells, tracheas were harvested, cleaned of attached connective tissue, and digested with 1.5 mg/mL Collagenase A (Roche), 0.4 mg/mL DNase I (Roche), and 2 U/mL Dispase II (Sigma–Aldrich) in HBSS at 37 °C for 30 min. Single-cell suspensions were washed, and approximately 5×10^5 cells per trachea were used for 11-color flow cytometry. Antibodies used included the following: CD45, CD11c, and IA/IE (eBioscience); CD11b and Ly6G (BD Biosciences); and F4/80, CD64, CD24, and CD31 (Biolegend). At least one channel was used for detecting autofluorescence. In addition, Invitrogen Aqua Live/Dead was used to exclude dead cells. Data were collected with a BD LSRII flow cytometer (BD Biosciences) and analyzed with FlowJo software (TreeStar, Inc.). For isolation of *Pdgfrα*-GFP cells and CD45$^+$ immune cells, tracheas from *Pdgfrα-H2B:GFP* mice were dissociated as described above. Cell suspensions were labeled with phycoerythrin-CD45 antibody, and cells were sorted using a FACSVantage SE system (Becton Dickinson). Statistical analysis was done using results from three different mice per condition.

Statistical Analysis. All results are mean ± SD. Statistical significance was determined by unpaired Student *t* tests unless otherwise described.

ACKNOWLEDGMENTS. We thank members of the B.L.M.H. laboratory for discussion, especially Christopher Vockley for advice on ChIP analysis,

Dr. Yen-Rei A. Yu for advice on FACs analysis, Danielle Hotten for assistance, and Dr. Ken Poss for critical comments on the manuscript. This work was supported by National Institutes of Health Grants U01-HL111018 (to B.L.M.H. and S.H.R.) DK065988 (to S.H.R.), and DA029925 (to L.S.B.).

1. Borthwick DW, Shahbazian M, Krantz QT, Dorin JR, Randell SH (2001) Evidence for stem-cell niches in the tracheal epithelium. *Am J Respir Cell Mol Biol* 24(6):662–670.
2. Rawlins EL, Ostrowski LE, Randell SH, Hogan BLM (2007) Lung development and repair: Contribution of the ciliated lineage. *Proc Natl Acad Sci USA* 104(2):410–417.
3. Rock JR, et al. (2011) Notch-dependent differentiation of adult airway basal stem cells. *Cell Stem Cell* 8(6):639–648.
4. Rock JR, et al. (2009) Basal cells as stem cells of the mouse trachea and human airway epithelium. *Proc Natl Acad Sci USA* 106(31):12771–12775.
5. Lai H, Rogers DF (2010) New pharmacotherapy for airway mucus hypersecretion in asthma and COPD: Targeting intracellular signaling pathways. *J Aerosol Med Pulm Drug Deliv* 23(4):219–231.
6. Randell SH (2006) Airway epithelial stem cells and the pathophysiology of chronic obstructive pulmonary disease. *Proc Am Thorac Soc* 3(8):718–725.
7. Guseh JS, et al. (2009) Notch signaling promotes airway mucous metaplasia and inhibits alveolar development. *Development* 136(10):1751–1759.
8. Tsao P-N, et al. (2009) Notch signaling controls the balance of ciliated and secretory cell fates in developing airways. *Development* 136(13):2297–2307.
9. Morimoto M, et al. (2010) Canonical Notch signaling in the developing lung is required for determination of arterial smooth muscle cells and selection of Clara versus ciliated cell fate. *J Cell Sci* 123(Pt 2):213–224.
10. Marcet B, et al. (2011) Control of vertebrate multiciliogenesis by miR-449 through direct repression of the Delta/Notch pathway. *Nat Cell Biol* 13(6):693–699.
11. Morimoto M, Nishinakamura R, Saga Y, Kopan R (2012) Different assemblies of Notch receptors coordinate the distribution of the major bronchial Clara, ciliated and neuroendocrine cells. *Development* 139(23):4365–4373.
12. Ma L, Quigley I, Omran H, Kintner C (2014) Multicilin drives centriole biogenesis via E2f proteins. *Genes Dev* 28(13):1461–1471.
13. Stubbs JL, Vladar EK, Axelrod JD, Kintner C (2012) Multicilin promotes centriole assembly and ciliogenesis during multiciliate cell differentiation. *Nat Cell Biol* 14(2): 140–147.
14. Tan FE, et al. (2013) Myb promotes centriole amplification and later steps of the multiciliogenesis program. *Development* 140(20):4277–4286.
15. Song R, et al. (2014) miR-34/449 miRNAs are required for motile ciliogenesis by repressing cp110. *Nature* 510(7503):115–120.
16. Wu J, et al. (2014) Two miRNA clusters, miR-34b/c and miR-449, are essential for normal brain development, motile ciliogenesis, and spermatogenesis. *Proc Natl Acad Sci USA* 111(28):E2851–E2857.
17. Waldner MJ, Foersch S, Neurath MF (2012) Interleukin-6—A key regulator of colorectal cancer development. *Int J Biol Sci* 8(9):1248–1253.
18. Hokuto I, et al. (2004) Stat-3 is required for pulmonary homeostasis during hyperoxia. *J Clin Invest* 113(1):28–37.
19. Kida H, et al. (2008) GP130-STAT3 regulates epithelial cell migration and is required for repair of the bronchiolar epithelium. *Am J Pathol* 172(6):1542–1554.
20. Kuhn C, 3rd, et al. (2000) Airway hyperresponsiveness and airway obstruction in transgenic mice. Morphologic correlates in mice overexpressing interleukin (IL)-11 and IL-6 in the lung. *Am J Respir Cell Mol Biol* 22(3):289–295.
21. Rock JR, Randell SH, Hogan BL (2010) Airway basal stem cells: A perspective on their roles in epithelial homeostasis and remodeling. *Dis Model Mech* 3(9-10):545–556.
22. Rincon M, Irvin CG (2012) Role of IL-6 in asthma and other inflammatory pulmonary diseases. *Int J Biol Sci* 8(9):1281–1290.
23. Chen J, Knowles HJ, Hebert JL, Hackett BP (1998) Mutation of the mouse hepatocyte nuclear factor/forkhead homologue 4 gene results in an absence of cilia and random left-right asymmetry. *J Clin Invest* 102(6):1077–1082.
24. You Y, Huang T (2004) Role of f-box factor foxj1 in differentiation of ciliated airway epithelial cells. *Am J Physiol Lung Cell Mol Physiol* 286(4):L650–L657.
25. Yu X, Ng CP, Habacher H, Roy S (2008) Foxj1 transcription factors are master regulators of the motile ciliogenic program. *Nat Genet* 40(12):1445–1453.
26. Ostrowski LE, Hutchins JR, Zakel K, O'Neal WK (2003) Targeting expression of a transgene to the airway surface epithelium using a ciliated cell-specific promoter. *Mole Ther* 8(4):637–645.
27. Takakura A, et al. (2011) Pyrimethamine inhibits adult polycystic kidney disease by modulating STAT signaling pathways. *Hum Mol Genet* 20(21):4143–4154.
28. Fulcher ML, Gabriel S, Burns KA, Yankaskas JR, Randell SH (2005) Well-differentiated human airway epithelial cell cultures. *Methods Mol Med* 107:183–206.
29. Wen Z, Zhong Z, Darnell JE, Jr (1995) Maximal activation of transcription by Stat1 and Stat3 requires both tyrosine and serine phosphorylation. *Cell* 82(2):241–250.
30. You Y, Richer EJ, Huang T, Brody SL (2002) Growth and differentiation of mouse tracheal epithelial cells: Selection of a proliferative population. *Am J Physiol Lung Cell Mol Physiol* 283(6):L1315–L1321.
31. Zhang S, Loch AJ, Radtke F, Egan SE, Xu K (2013) Jagged1 is the major regulator of Notch-dependent cell fate in proximal airways. *Dev Dynamics* 242(6):678–686.
32. Laoukili J, et al. (2001) IL-13 alters mucociliary differentiation and ciliary beating of human respiratory epithelial cells. *J Clin Invest* 108(12):1817–1824.
33. Gomperts BN, Kim LJ, Flaherty SA, Hackett BP (2007) IL-13 regulates cilia loss and foxj1 expression in human airway epithelium. *Am J Respir Cell Mol Biol* 37(3):339–346.
34. O'Shea JJ, Murray PJ (2008) Cytokine signaling modules in inflammatory responses. *Immunity* 28(4):477–487.
35. Li Z, Burns AR, Miller SB, Smith CW (2011) CCL20, gammadelta T cells, and IL-22 in corneal epithelial healing. *FASEB J* 25(8):2659–2668.
36. Hamilton TG, Klinghoffer RA, Corrin PD, Soriano P (2003) Evolutionary divergence of platelet-derived growth factor alpha receptor signaling mechanisms. *Mol Cell Biol* 23(11):4013–4025.
37. Neveu WA, et al. (2011) Fungal allergen β-glucans trigger p38 mitogen-activated protein kinase-mediated IL-6 translation in lung epithelial cells. *Am J Respir Cell Mol Biol* 45(6):1133–1141.
38. Scheller J, Chalaris A, Schmidt-Arras D, Rose-John S (2011) The pro- and anti-inflammatory properties of the cytokine interleukin-6. *Biochim Biophys Acta* 1813(5):878–888.
39. Jiang H, et al. (2009) Cytokine/Jak/Stat signaling mediates regeneration and homeostasis in the Drosophila midgut. *Cell* 137(7):1343–1355.
40. Lin G, Xu N, Xi R (2010) Paracrine unpaired signaling through the JAK/STAT pathway controls self-renewal and lineage differentiation of drosophila intestinal stem cells. *J Mol Cell Biol* 2(1):37–49.
41. Resende LP, Jones DL (2012) Local signaling within stem cell niches: Insights from Drosophila. *Curr Opin Cell Biol* 24(2):225–231.
42. Choksi SP, Lauter G, Swoboda P, Roy S (2014) Switching on cilia: Transcriptional networks regulating ciliogenesis. *Development* 141(7):1427–1441.
43. Montefort S, Roche WR, Holgate ST (1993) Bronchial epithelial shedding in asthmatics and non-asthmatics. *Resp Med* 87(Suppl B):9–11.
44. Hawkins GA, et al. (2012) The IL6R variation Asp(358)Ala is a potential modifier of lung function in subjects with asthma. *J Allergy Clin Immunol* 130(2):510–515 e511.
45. Ferreira MA, et al.; Australian Asthma Genetics Consortium (2011) Identification of IL6R and chromosome 11q13.5 as risk loci for asthma. *Lancet* 378(9795):1006–1014.
46. Croker BA, et al. (2003) SOCS3 negatively regulates IL-6 signaling in vivo. *Nat Immunol* 4(6):540–545.
47. Van Keymeulen A, et al. (2011) Distinct stem cells contribute to mammary gland development and maintenance. *Nature* 479(7372):189–193.
48. Srinivas S, Watanabe T (2001) Cre reporter strains produced by targeted insertion of EYFP and ECFP into the ROSA26 locus. *BMC Dev Biol* 1:4.
49. Suprynowicz FA, et al. (2012) Conditionally reprogrammed cells represent a stem-like state of adult epithelial cells. *Proc Natl Acad Sci USA* 109(49):20035–20040.
50. Takahashi K, Yamanaka S (2006) Induction of pluripotent stem cells from mouse embryonic and adult fibroblast cultures by defined factors. *Cell* 126(4):663–676.
51. Wen Z, Darnell JE, Jr (1997) Mapping of Stat3 serine phosphorylation to a single residue (727) and evidence that serine phosphorylation has no influence on DNA binding of Stat1 and Stat3. *Nucleic Acids Res* 25(11):2062–2067.

Supporting Information

Tadokoro et al. 10.1073/pnas.1409781111

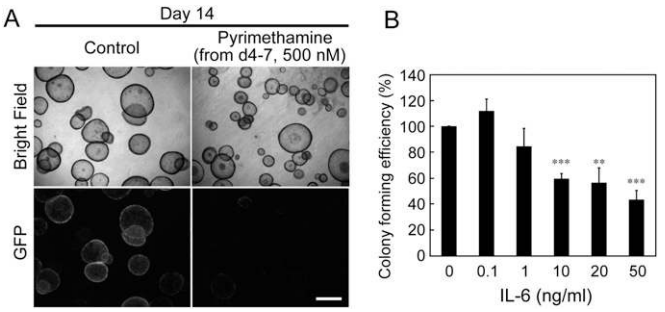

Fig. S1. Related to Fig. 1. (*A*) Effect of pyrimethamine, a Stat3 inhibitor, on forkhead box protein J1 (*Foxj1*)-GFP expression in spheres. Differential interference contrast images (*Upper*) and fluorescent images of the same spheres (*Lower*) are shown. d, day(s). (*B*) Colony-forming efficiencies at different doses of IL-6. Error bars indicate SD. $^{**}P < 0.01$ against control; $^{***}P < 0.001$ against control ($n = 3$). (Scale bar: 500 μm.)

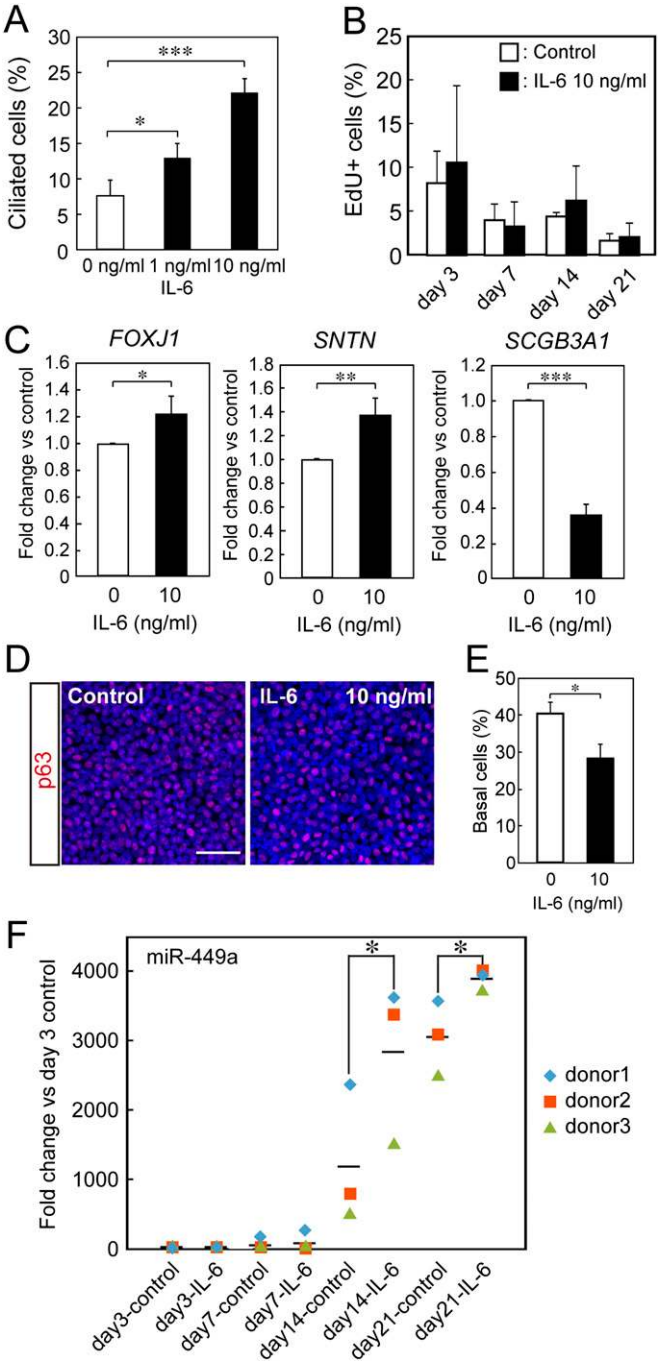

Fig. S2. Related to Fig. 2. (*A*) Effect of IL-6 on ciliogenesis in human air–liquid interface (ALI) culture. Primary human bronchial epithelial cells from three donors were cultured on inserts for 21 d with or without IL-6 (0, 1, and 10 ng/mL). Inserts were stained in whole mounts for α-tubulin (ciliated cells, green) and counterstained with DAPI. Ciliated cells were quantified as a percentage of total DAPI$^+$ cells. Error bars indicate SD. *$P < 0.05$ against control; ***$P < 0.001$ against control ($n = 3$). (*B*) 5-ethynyl-2′-deoxyuridine$^+$ cells were quantified in control and IL-6 (10 ng/mL)–treated ALI culture from three donors as a percentage of total DAPI$^+$ cells at day 3, day 7, day 14, and day 21. (*C*) Quantitative RT-PCR shows that IL-6 treatment up-regulates ciliogenesis-related genes, such as *FOXJ1* and Sentan (*SNTN*), and down-regulates secretory cell-related gene *secretoglobin 3A1* (*SCGB3A1*) in human ALI culture. The expression levels were normalized to the control hypoxanthine phosphoribosyltransferase 1 (*HPRT1*). Error bars indicate SD. *$P < 0.05$ against control; **$P < 0.01$ against control; ***$P < 0.001$ against control ($n = 3$). (*D*) Whole-mount staining of day 21 human ALI cultures for basal cells (p63, red). Nuclei are blue (DAPI). (Scale bar: 40 μm.) (*E*) Quantification of *D* as a percentage of total DAPI$^+$ cells. Values are mean and SEM for cultures from three different donors. Error bars indicate SD. *$P < 0.05$ against control ($n = 3$). (*F*) RNA was extracted from ALI cultures from three different donors with or without IL-6 (10 ng/mL) at day 3, day 7, day 14, and day 21 and subjected to quantitative RT-PCR analysis. The expression level of miR-449a, a microRNA which controls ciliogenesis, was normalized to the control gene ribosomal protein L21. Statistical significance was determined by the paired Student *t* test. Error bars indicate SD. *$P < 0.05$ against control ($n = 3$).

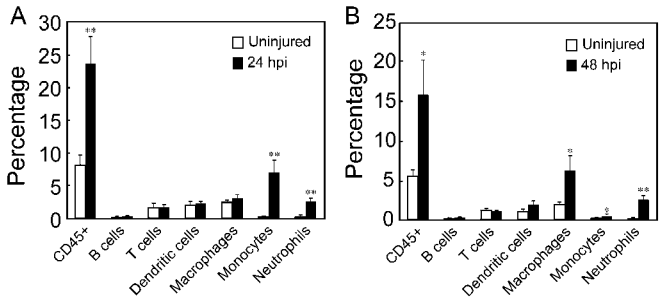

Fig. S3. Related to Fig. 6. (*A*) Immune cell populations in the trachea from three different mice were analyzed by fluorescence-activated cell sorting (FACS) and quantified as a percentage of live cells after SO_2 injury at 24 h postinjury (hpi). Error bars indicate SD ($n = 3$). (*B*) Immune cell populations in trachea from three different mice were analyzed by FACS and quantified as a percentage of live cells after SO_2 injury at 48 hpi. Error bars indicate SD ($n = 3$). $^*P < 0.05$ against uninjured trachea; $^{**}P < 0.01$ against uninjured trachea ($n = 3$).

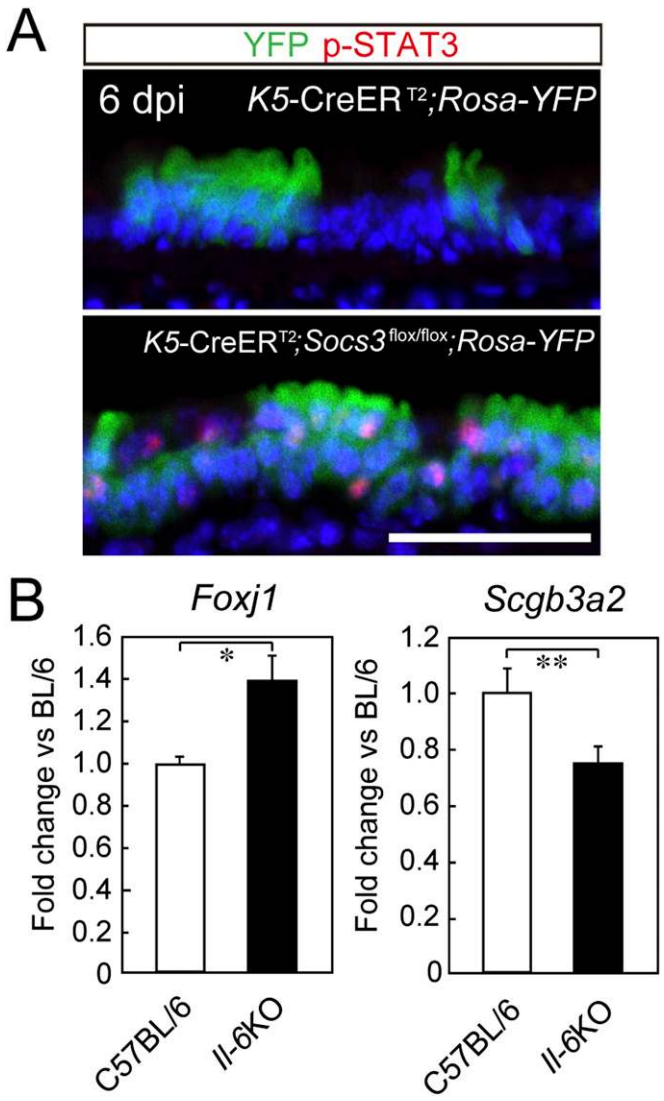

Fig. S4. Related to Fig. 7. (*A*) Expression of phospho-STAT3 (p-STAT3; red) and YFP (green) at 6 d after SO_2 injury in control trachea [*Upper*; *Keratin 5* (*K5*)-*CreER^{T2}; Rosa-YFP*] and a gain-of-function model [*Lower*; *K5-CreER^{T2}; suppressor of cytokine signals 3* (*Socs3*)$^{flox/flox}$; *Rosa-YFP*]. Note the persistence of p-STAT3$^+$ nuclei in the epithelial cells in which the feedback inhibitor, Socs3, is conditionally deleted. (Scale bar: 50 μm.) (*B*) Quantitative RT-PCR analysis shows reduced *Foxj1* expression and increased *secretoglobin 3a2* (*Scgb3a2*) expression in *Il-6* null mice compared with C57BL/6 mice after SO_2 injury (4 d postinjury). The expression levels were normalized to the control *Hprt1*. Error bars indicate SD. $^*P < 0.05$ against control; $^{**}P < 0.01$ against control ($n = 3$).

Table S1. Primers for quantitative PCR

	Forward	Reverse
Il-6	5′-GAGGATACCACTCCCAACAGACC-3′	5′-AAGTGCATCATCGTTGTTCATACA-3′
Il-10	5′-GGTTGCCAAGCCTTATCGGA-3′	5′-GGGATCACAGGTTGGTCTG-3′
Il-11	5′-GACTCTGGAGCCAGAGCTG-3′	5′-GGGATCACAGGTTGGTCTG-3′
Cntf	5′-CCATCCACTGAGTCAAGGCT-3′	5′-TGGCTAGCAAGGAAGATTCG-3′
Lif	5′-AGCAGCAGTAAGGGCACAAT-3′	5′-CCCCATTTGAGCATGAACTT-3′
Osm	5′-CCATGCTCAGGATGAGGAGA-3′	5′-AGCTGTGTCACCCCTGAGAG-3′
Gapdh	5′-AGGTCGGTGTGAACGGATTTG-3′	5′-TGTAGACCATGTAGTTGAGGTCA-3′
Hprt1	5′-GAGGAGTCCTGTTGATGTTGCCAG-3′	5′-GGCTGGCCTATAGGCTCATAGTGC-3′
Socs3	5′-AACTTGCTGTGGGTGACCAT-3′	5′-AAGGCCGGAGATTTCGCT-3′
Foxj1	5′-CAACTTCTGCTACTTCCGCC-3′	5′-CGAGGCACTTTGATGAAGC-3′
Mcidas	5′-AAGAGTTGGTTTGCGTGCTT-3′	5′-ACCCCAGGACTGGAGTTTCT-3′
Cdc20b	5′-GAAGGAAAATCTTGCCACCA-3′	5′-CATCTTCCCATCGATTTGCT-3′
Notch1	5′-TGTTGTGCTCCTGAAGAACG-3′	5′-GCAACACTTTGGCAGTCTCA-3′
Notch2	5′-ATGTGGACGAGTGTCTGTTGC-3′	5′-GGAAGCATAGGCACAGTCATC-3′
Dll1	5′-CCGGCTGAAGCTACAGAAAC-3′	5′-AGCCCCAATGATGCTAACAG-3′
Jagged1	5′-CCTCGGGTCAGTTTGAGCTG-3′	5′-CCTTGAGGCACACTTTGAAGTA-3′
Scgb3a2	5′-CCAAAGTCCCGGAAAACATC-3′	5′-AGGGCAGTGGCAGAATAACC-3′
FOXJ1	5′-GTTTGGGTTTGGTGGTTTGG-3′	5′-TGGTCCCAGTAGTTCCAGCA-3′
SNTN	5′-TTGCCACCACTGCTCTGATT-3′	5′-GGCTTGGTTTCTTGTCCCTCT-3′
SCGB3A1	5′-CATAGAGGGCTCCCAGAAGTG-3′	5′-CAGCGTCTTGTCCTCAGGTG-3′
HPRT1	5′-TGTCAGTTGCTGCATTCCTAAA-3′	5′-TAAACAACAATCCGCCCAAA-3′

Cdc20b, cell division cycle 20B; *Cntf*, ciliary neurotrophic factor; *Dll1*, delta-like 1; *Foxj1*/*FOXJ1*, forkhead box protein J1; *Hprt1*/*HPRT1*, hypoxanthine phosphoribosyltransferase 1; *Lif*, leukemia inhibitory factor; *Mcidas*, multicilin; *Osm*, oncostatin-M; *SCGB3A1*, secretoglobin 3A1; *Scgb3a2*, secretoglobin 3a2; *SNTN*, sentan; *Socs3*, suppressor of cytokine signals 3.